Journal Name

ARTICLE

Hyperbranched poly(ethylenimine-*co*-oxazoline) by thiol-yne chemistry for non-viral gene delivery: investigating the role of polymer architecture

Received 00th January 20xx,
Accepted 00th January 20xx

DOI: 10.1039/x0xx00000x

www.rsc.org/

Alexander B. Cook,[1] Raoul Peltier,[1] Junliang Zhang,[1] Pratik Gurnani,[1] Joji Tanaka,[1] James A. Burns,[2] Robert Dallmann,[3] Matthias Hartlieb,[1‡*] and Sébastien Perrier[1,3,4*]

Cationic polymers have been widely employed as gene delivery vectors to help circumvent extracellular and intracellular delivery barriers. Among them, polyethylenimine (PEI) is the most commonly used despite its associated high cytotoxicity. PEI is typically obtained by uncontrolled ring opening polymerisation of aziridine, leading to either linear polymer architectures with only secondary amines, or branched architectures containing primary, secondary, and tertiary amines. In contrast, we describe the preparation of hyperbranched poly(ethylenimine-*co*-oxazoline) that contains only secondary amines, *via* a fast thiol-yne based one pot reaction. A small library of these compounds with varying PEI contents was then used to study the effect of polymer architecture on pDNA polyplex formation, cytotoxicity, and *in vitro* transfection studies with plasmid DNA. Hyperbranched poly(ethylenimine-*co*-oxazoline) was found to have reduced toxicity compared to the commercial standard 25K branched PEI (bPEI), with transfection efficiencies only slightly lower than its bPEI counterpart. Obtained results highlight the importance of the polymer architecture on the transfection efficiency of a gene delivery system, which was demonstrated by excluding other parameters such as molecular weight and charge density.

Introduction

Gene therapy is an important and hugely promising pharmaceutical development that aims to treat diseases by delivering genetic material or recombinant DNA to target cells.[1,2] In the clinic, this can take the form of replacing, adding, or editing a gene that is absent or abnormal and which is responsible for a disease. This technique opens the door for treatment of a number of previously undruggable targets. The versatility of gene therapy makes it relevant for a wide variety of diseases, including different type of cancers, Parkinson's disease, cystic fibrosis, macular degeneration, and muscular dystrophy among others.[3-7] In recent years, the potential impact of gene therapy has been expanded even further by the development of CRISPR/Cas9 gene editing technology.[8,9]

Since the early genetic engineering studies in the 1970s, the major hurdle associated with gene delivery lies in effectively delivering the genetic material inside target cells.[2] This is typically achieved using either viral vectors or synthetic non-viral vectors. Viral vectors, such as retroviruses, adenoviruses, or adeno-associated viruses (AAVs) have the advantage of providing higher transgene expression but are typically limited by immunogenicity and safety-related issues, packaging constraints, as well as the requirement of cell mitosis.[10] Comparatively, non-viral gene delivery vectors offer access to large scale production, low host immunogenicity, easily tuneable architecture/functionality, long term storage stability, and batch to batch reproducibility of materials. Commonly used synthetic vectors include cationic polymers, liposomes, and covalent polymer conjugates.[10-12] Cationic polymers such as poly-L-lysine (PLL), polyethylenimine (PEI), poly(2-(dimethylamino)ethyl methacrylate) (PDMAEMA), and polyamidoamine dendrimers (PAMAM) are promising systems for the non-viral trafficking of genetic material. Despite their popularity, high cytotoxicity associated with their polycationic nature, which tends to cause disruption of cellular membranes, remains a major limitation.[10]

The current gold-standard when referring to polymeric non-viral gene delivery systems is bPEI. Reports indicate that polymer molecular weight plays an important role in achieving optimal gene transfection.[13] However, these systems are notoriously difficult to characterise and there is still much debate about the individual influence of polymer molecular weight and architecture on the transfection efficiency and toxicity of the resulting polyplexes.[14-17] Problems arise from difficulties in synthesising comparable polymer systems with

[1] *Department of Chemistry, University of Warwick, Coventry, CV4 7AL, UK*
[2] *Syngenta, Jealott's Hill International Research Centre, Bracknell, Berkshire, RG42 6EY, UK*
[3] *Warwick Medical School, University of Warwick, Coventry, CV4 7AL, UK*
[4] *Faculty of Pharmacy and Pharmaceutical Sciences, Monash University, 381 Royal Parade, Parkville, Victoria 3052, Australia*
[‡] *Current address: Institute of Biomaterial Science, Helmholtz-Zentrum Geesthacht, Teltow, Germany*
**Corresponding author: Email: s.perrier@warwick.ac.uk, matthias.hartlieb@hzg.de*

Electronic Supplementary Information (ESI) available: [details of any supplementary information available should be included here]. See DOI: 10.1039/x0xx00000x

differing architectures, without affecting several properties of the polymers at once. The importance of controlling branching in polyplex formation was demonstrated by Tang *et al.*, who showed that semi-degraded PAMAM dendrimers provide better transfection efficiency in comparison with whole PAMAM dendrimers.[18] In the case of bPEI, which is commonly prepared via uncontrolled ring-opening polymerisation of aziridine, the nature and frequency of the branching points are uncontrolled and highly dependent on the reaction conditions. In addition, the resulting polymer consists of a mixture of primary, secondary, and tertiary amines, whose pK_a values, and hence ability to interact with genetic material or membranes differ significantly.[19]

An alternative route to preparing PEI uses cationic ring-opening-polymerisation of 2-oxazolines, followed by a hydrolysis step. The method allows preparation of polymers containing only secondary amines, with a defined molecular weight and well-controlled molecular weight distribution. This approach was used by Wightman *et al.* to demonstrate that branched and linear PEI differed in their ability to transfect cells, both *in vitro* and *in vivo*.[17] In 2015, the Grayson group prepared cyclic PEI and the exact linear equivalent and studied the effect of cyclic architecture on transfection efficiency and cytotoxicity.[20]

Over the past few years, our group has developed thiol-yne chemistry as a strategy to synthesise hyperbranched polymers with remarkably high degrees of branching and tuneable functionality.[21-24] Hyperbranched polymers from AB_2 monomers have received increasing interest due to a number of unique features including globular three dimensional conformations and high number of surface functionalities. The thiol-yne chemistry allows fast one pot synthesis of hyperbranched polymers with degrees of branching similar to that of perfectly branched dendrimers. Such control over the branching process is attributed to the reactive nature of pi bonds to thiyl radical additions. Recently, the Schubert group has reported the synthesis of poly(ethylenimine-*co*-oxazoline) copolymers and their application as gene delivery vectors.[25,26] The copolymers show reduced toxicity as compared to linear PEI homopolymers and incorporation of 'stealth' properties including reduced non-specific interactions with serum and other biological compounds.[27] However, the lack of access to more complex architectures, such as branched structures, has so far limited the potential application of these copolymers.

The aim of this study is to investigate the influence of polymer architecture on the transfection ability of the macromolecules. Consequently, we seek to isolate the impact of polymer structure (hyperbranched vs. linear) while maintaining other key elements such as molecular weight, charge density or nature of the repeating unit. This contribution describes the combination of thiol-yne chemistry with well-defined poly(ethylenimine-*co*-oxazoline) copolymers, which allows synthesis of hyperbranched PEI containing only secondary amines for the first time. The article then moves onto a systematic study of this novel polymer architecture, including comparison with a precise linear equivalent, as well as comparison with commercially available bPEI. The polymers were then evaluated for their performance as non-viral gene delivery vectors. Results include plasmid DNA complexation ability, polyplex morphology, buffering capacity, polymer cytotoxicity, and gene transfection efficiency *in vitro* using a green fluorescent protein (GFP) encoding reporter plasmid.

Experimental

Materials

Propargyl tosylate, methyl tosylate (MeTos), potassium ethyl xanthogenate, 2-ethyl-2-oxazoline (EtOx), dimethylamine (33% in ethanol), 2,2-dimethoxy-2-phenylacetophenone (DMPA), ethidium bromide (EtBr), polyethylenimine branched (bPEI, Mw ~25,000 by LS, Mn ~10,000 by SEC) were obtained from Sigma-Aldrich. All other materials were purchased from Fisher Scientific, or Sigma-Aldrich. Green fluorescent protein (GFP) expressing plasmid DNA (pWPI) was a gift from Didier Trono (Addgene plasmid # 12254). 2-Ethyl-2-oxazoline (EtOx) and methyl tosylate (MeTos) were distilled to dryness prior to use. EtOx was dried using CaH_2 before distillation. 50X Tris-Acetate-EDTA (TAE) buffer for gel electrophoresis was made up at concentration of 2.0M Tris acetate (Sigma Aldrich) and 0.05M EDTA (Sigma Aldrich) in deionised water, pH 8.2 - 8.4 and stored at room temperature. Agarose loading buffer for samples (colourless) were made up at 30% (vol/vol) glycerol (Sigma Aldrich) in deionised water and stored at room temperature.

Characterisation

Size Exclusion Chromatography (SEC) was performed in DMF, using an Agilent 390-LC MDS instrument equipped with differential refractive index (DRI), viscometry, dual angle light scattering, and dual wavelength UV detectors. The system was equipped with 2 x PLgel Mixed D columns (300 x 7.5 mm) and a PLgel 5 µm guard column. The eluent was DMF with 5 mmol NH_4BF_4 additive, and samples were run at 1 mL/min at 50 °C. Analyte samples were filtered through a nylon membrane with 0.22 µm pore size before injection. Apparent molar mass values ($M_{n,SEC}$ and $M_{w,SEC}$) and dispersity ($Đ$) of synthesized polymers were determined by DRI detector and conventional calibration using Agilent SEC software. Poly(methyl methacrylate) (PMMA) standards (Agilent EasyVials) were used for calibration. The Kuhn-Mark-Houwink-Sakurada parameter α, relating to polymer conformation in solution was determined from the gradient of the double logarithmic plot of intrinsic viscosity as a function of molecular weight, using the SEC viscometry detector and Agilent SEC software. Proton nuclear magnetic resonance spectra (^{1}H NMR) were recorded on a Bruker Advance 400 spectrometer (400 MHz) at 27 °C, with chemical shift values (δ) reported in ppm, and the residual proton signal of the solvent used as internal standard. Proton-decoupled carbon nuclear magnetic resonance spectra (^{13}C NMR) were recorded on a Bruker Advance 400 spectrometer (100 MHz) at 27 °C, with chemical shift values (δ) reported in ppm, and the residual proton signal of the solvent used as internal standard. Fourier transform infrared spectra (FTIR) were recorded on a Bruker

Alpha FTIR ATR. Electrospray ionisation time-of-flight mass spectra (ESI-MS) were recorded using a Bruker MicroToF.

Oxazoline polymerisation

For a typical polymerisation, dry 2-ethyl-2-oxazoline (7.93 g, 80 mmol), propargyl tosylate (1.68 g, 8 mmol), and acetonitrile (10.54 mL) were added to a Schlenk flask under nitrogen and left to stir in an oil bath at 80 °C. After a predetermined time, the solution was removed from the oil bath, a sample for the determination of the conversion was taken, and a solution of potassium ethyl xanthate (1.54 g, 9.6 mmol) was added to terminate the polymer chain. The product was left to stir for 1 h before being diluted with chloroform (100 mL). The organic layer was then washed with sat. Na_2CO_3 (3 × 100 mL) and brine (3 × 100 mL), and then dried over $MgSO_4$. The chloroform was removed to leave a colourless oil. The oil was re-dissolved in DCM (10 mL), precipitated into ether, the polymer was collected by gravity filtration as a white solid and then dried under vacuum. ^{1}H NMR spectrum shown in Figure S1. Propargyl-pEtOx-xanthate (1.1 g, 1.38 mmol) was dissolved in dimethylamine (33% in EtOH) (12 mL) deoxygenated with nitrogen bubbling and stirred at 40 °C for 3 h. The reaction mixture was then poured over a solution of sulphuric acid (H_2SO_4) (8 mL) and ice-water (80 mL). The polymer was extracted by washing with $CHCl_3$ (3 × 50 mL), followed by washing of the $CHCl_3$ layer with sat. Na_2CO_3 (2 × 50 mL) and brine (2 × 50 mL). The organic layer was then dried over $MgSO_4$ and filtered before the solvent was removed to yield the thiol-yne poly(oxazoline) macromonomer which was stored under nitrogen to reduced chance of disulfide formation. M_n = 1,200 g/mol, $Đ$ = 1.19 (DMF SEC, + NH_4BF_4 additive eluent, PMMA calibration). ^{1}H NMR spectrum shown in Figure S2. Full functionalisation of both chain ends was confirmed using ESI-MS. ^{1}H NMR spectrum (400 MHz, $CDCl_3$, δ ppm): 4.12 (2H, -C**H$_2$**-C≡CH), 3.40-3.60 (4H, N-C**H$_2$**-C**H$_2$**-N), 2.25-2.45 (2H, NC(O)-C**H$_2$**-CH_3), 1.05-1.20 (3H, NC(O)-CH_2-C**H$_3$**). ^{13}C NMR spectrum (100 MHz, $CDCl_3$, δ ppm): 174.51 (N**C**(O)), 73.41 (-**C**≡CH), 70.46 (-C≡**C**H), 45.3 (N-**C**H$_2$-**C**H$_2$-N), 25.90 (NC(O)-**C**H$_2$-CH_3), 13.75 (-**C**H$_2$-SH), 9.39 (NC(O)-CH_2-**C**H$_3$). FTIR ν cm^{-1}: 3491 (broad, N-H amide), 3270-3290 (weak, ≡C-H alkyne), 2980 (medium, C-H alkane), 2835 (weak, N-CH_2- amine), 1624 (strong, C=O amide I), 1418 (medium, N-H amide II). The linear control poly(oxazoline) was synthesised in the same manner using methyl tosylate as the initiator and termination under ambient humid conditions. The ^{1}H NMR spectrum is shown in Figure S4 and S5, SEC chromatogram is shown in Figure S3, M_n = 13,700 g/mol, $Đ$ = 1.25 (DMF SEC, DRI detector).

Thiol-yne polymerisation

A typical polymerisation is as follows: thiol-yne macromonomer (600 mg, 0.75 mmol) was dissolved with DMPA (90 mg, 0.352 mmol) in DMF (2.5 mL) in a vial equipped with a small stirrer bar and a rubber septum screw cap. Monomer to initiator ratio was kept the same for all polymerisations. The vial was wrapped in aluminium foil and deoxygenated with nitrogen for 5 min. The vial was placed under a 365 nm UV lamp (UVP, UVGL-55, 6 watt, 365 nm) in an aluminium foil lined dark box over a magnetic stirrer plate. For the kinetic samples, each time point corresponds to a separate vial removed after the allocated polymerisation time. After the predetermined reaction time, the vial was removed and analysed by SEC. Polymer reaction mixture was precipitated in diethyl ether and the polymer recovered by centrifugation. M_w = 14,000 g/mol, $Đ$ = 1.5 (DMF SEC, DRI detector). ^{1}H NMR spectrum (400 MHz, $CDCl_3$, δ ppm): 5.60-6.20 (2H, -C**H**=C**H**-, weak), 3.95 (2H, -C**H$_2$**-C≡CH, weak), 3.40-3.55 (4H, N-C**H$_2$**-C**H$_2$**-N), 2.15-2.40 (2H, NC(O)-C**H$_2$**-CH_3), 0.90-1.20 (3H, NC(O)-CH_2-C**H$_3$**). ^{13}C NMR spectrum (100 MHz, $CDCl_3$, δ ppm): 174.59 (N**C**(O)), 45.41 (N-**C**H$_2$-**C**H$_2$-N), 25.90 (NC(O)-**C**H$_2$-CH_3), 9.30 (NC(O)-CH_2-**C**H$_3$). FTIR ν cm^{-1}: 3490 (broad, N-H amide), 3270-3290 (weak, ≡C-H alkyne), 2976 (medium, C-H alkane), 2830 (weak, N-CH_2- amine), 1621 (strong, C=O amide I), 1425 (medium, N-H amide II).

Hydrolysis of PEtOx

The hydrolysis kinetics were performed in a microwave synthesiser (Biotage Initiator+ Eight). Hydrochloric acid (0.025 mL, 36 wt%) solution was mixed with 0.275 mL of PEtOx stock solution, giving a total volume in each vial (0.5 mL microwave vial) of 0.3 mL with a concentration of 1 M HCl. The vials were heated at 120 °C for varying reaction times. The reaction mixtures were cooled down by compressed air and made basic with 0.1 mL of a 4 M NaOH solution to a pH of 8-9, and freeze dried for ^{1}H NMR spectroscopy. The conversion was calculated from the ^{1}H NMR spectra signals of the hydrolysis products in deuterated methanol. Spectra can be found in Figure S8-S9. All signals described for PEtOx are present, together with the signals corresponding to the respective hydrolysis products. The dried crude polymer was then redissolved in water and dialysed against a 0.5 - 1 kDa membrane to remove propionic acid salts, and then freeze dried. Final poly(ethylenimine-*co*-2-ethyl-2-oxazoline) copolymer compositions were calculated from the appropriate backbone signals from the ^{1}H NMR spectra of the purified polymers. Once the kinetics of the hydrolysis had been established the hydrolysis was scaled up to 20 mL microwave vials, to obtain the appropriate polymers for the rest of the studies. For a typical ethylenimine oxazoline copolymer: ^{1}H NMR spectrum (400 MHz, $CDCl_3$, δ ppm): 3.45-3.71 (4H, N-C**H$_2$**-C**H$_2$**-N (POx)), 2.75-2.92 (4H, N-C**H$_2$**-C**H$_2$**-N (PEI)), 2.31-2.55 (2H, NC(O)-C**H$_2$**-CH_3), 1.04-1.20 (3H, NC(O)-CH_2-C**H$_3$**). ^{13}C NMR spectrum (100 MHz, $CDCl_3$, δ ppm): 174.59 (N**C**(O)), 45.41 (N-**C**H$_2$-**C**H$_2$-N), 25.90 (NC(O)-**C**H$_2$-CH_3), 9.30 (NC(O)-CH_2-**C**H$_3$). FTIR ν cm^{-1}: 3484 (broad, N-H amide), 3282 (broad, N-H amine secondary), 2987 (medium, C-H alkane), 2833 (weak, N-CH_2-amine), 1624 (strong, C=O amide I), 1420 (medium, N-H amide II).

Cell culture and polymer toxicity

HEK293T cells were cultured in DMEM supplemented with 10% fetal bovine serum, 2 mM glutamine and 1% penicillin/streptomycin. The cells were grown as adherent monolayers at 310 K under a 5% CO2 humidified atmosphere and passaged at approximately 70–80% confluence. For polymer toxicity evaluation, HEK293T cells were seeded in a 96 well plate at a density of 1 × 10^4 cells per well. After 16 hours, the culture medium was replaced by fresh media containing a series of dilution of the polymers (2, 0.8, 0.2, 0.08, 0.02 mg/mL), prepared from stock solutions in PBS. Following 24 h incubation, the medium was removed, cells washed

Scheme 1. Preparation of AB_2 poly(2-ethyl-2-oxazoline) thiol-yne macromonomer and subsequent batch photopolymerisation to from hyperbranched poly(2-ethyl-2-oxazoline).

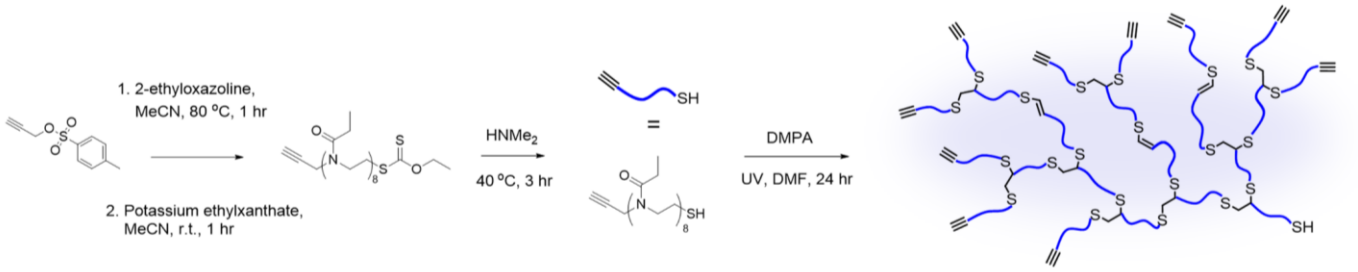

with PBS, and media replaced with fresh medium and 25 µL of a solution of XTT (1 mg mL^{-1}) containing N-methyl dibenzopyrazine methyl sulfate (PMS) (25 µmol L^{-1}) in medium was added. Cells were further incubated for 16 h. Absorbance of the samples was finally measured using a plate reader at 450 nm and 650 nm. The data presented are representative of a minimum of two independent experiments where each sample was measured in triplicate. Errors reported correspond to the standard deviation of the mean.

***In vitro* transfection**

Polyplex samples were prepared prior to incubation with the cells, *via* mixing of plasmid DNA solution (final $concentration_{DNA}$ = 100 µg/mL) with the appropriate amount of polymer predissolved in sterile water (N/P ratio = 20), and left to complex at room temperature for one hour. HEK293T cells were seeded in a 24 well plate at a density of 1×10^5 cells per well. After 16 hours, the culture medium was replaced by Optimem® cell culture media (Thermo Fisher Scientific) without fetal bovine serum. After one hour, the media was replaced by fresh Optimem® media containing the polyplex solutions (final $concentration_{DNA}$ = 10 µg/mL), the cells left to incubate for 5 hours under 5% CO_2 humidified atmosphere, then the media replaced with fresh culture media containing fetal bovine serum. Following 24 hours incubation, cells were washed with PBS, trypsinised, centrifuged, re-dispersed in ice-cold PBS and filtered into FACS tubes for analysis. Intracellular fluorescence was quantified using a BD LSR II cytometer (BD Biosciences) at excitation 488 nm and emission 525 nm. The geometric mean fluorescence was used as the sample value. The data in presented are representative of two separate experiments where each sample was measured in duplicate (n = 4). All errors reported correspond to the standard deviation from the mean.

Results and Discussion

Hyperbranched poly(ethylenimine-*co*-2-ethyl-2-oxazoline) copolymers

The thiol-yne macromonomer used for the formation of hyperbranched poly(2-ethyl-2-oxazoline) (PEtOx) was prepared following a two-step process (**Scheme 1**). Firstly, cationic ring opening polymerisation (CROP) was employed to polymerise 2-ethyl-2-oxazoline (EtOx) in acetonitrile at 80 °C, using propargyl tosylate as an initiator and potassium ethyl xanthate as nucleophilic end-capping agent. This afforded separate functionalities at both ends of the polymer chains, an alkyne functional α-chain end and a protected thiol functional ω-chain end, whilst maintaining well-defined molecular weights and low dispersity values. To ensure a high end group fidelity, a degree of polymerisation (DP) of 10 was targeted for the PEtOx precursor.

From the ^{1}H NMR spectrum of the polymerisation mixture, a DP of 8 was determined by comparing the methylene signals of the propargyl group with the signal of the polymer backbone (**Figure S1**). This value compares well with the value obtained by SEC (M_n = 1200 g/mol, $Đ$ = 1.19). After purification, ^{1}H-NMR spectroscopy was used to determine the degree of functionalisation for both end groups. In both cases the degree of functionalisation was found to be higher than 95%. In order to generate the thiol end group on the PEtOx chains, aminolysis of the xanthate group was carried out in the presence of dimethylamine. ^{1}H-NMR spectroscopy shows the complete disappearance of the peaks associated with the xanthate group. The presence of the thiol end group was confirmed using electrospray ionisation mass spectrometry (ESI-MS) of the macromonomer, which showed a single distribution corresponding to PEtOx with alkyne and thiol chain-ends (**Figure 1a**).

The telechelic thiol-yne PEtOx macromonomers were then polymerised following a procedure depicted in **Scheme 1**. The polymerisation proceeded under UV light irradiation using 0.5 equivalents of photoinitiator DMPA per macromonomer chain. A macromonomer concentration of 0.3 M in DMF was chosen according to an initial polymerisation optimisation study, in order to obtain high molecular weights suitable for transfection (**Figure S6** and **Table S1**). The inherent reactivity of pi bonds to thiyl radicals, which proceeds *via* a two-step mechanism, is expected to result in very high degrees of branching in the final compounds. Bowman *et al.* showed that the second addition of a thiyl radical to a vinylthioether species proceeds much faster that the first addition of a thiyl radical to an alkyne.[28] Therefore, most thiol-yne photo-additions proceed to the fully branched dendritic species.

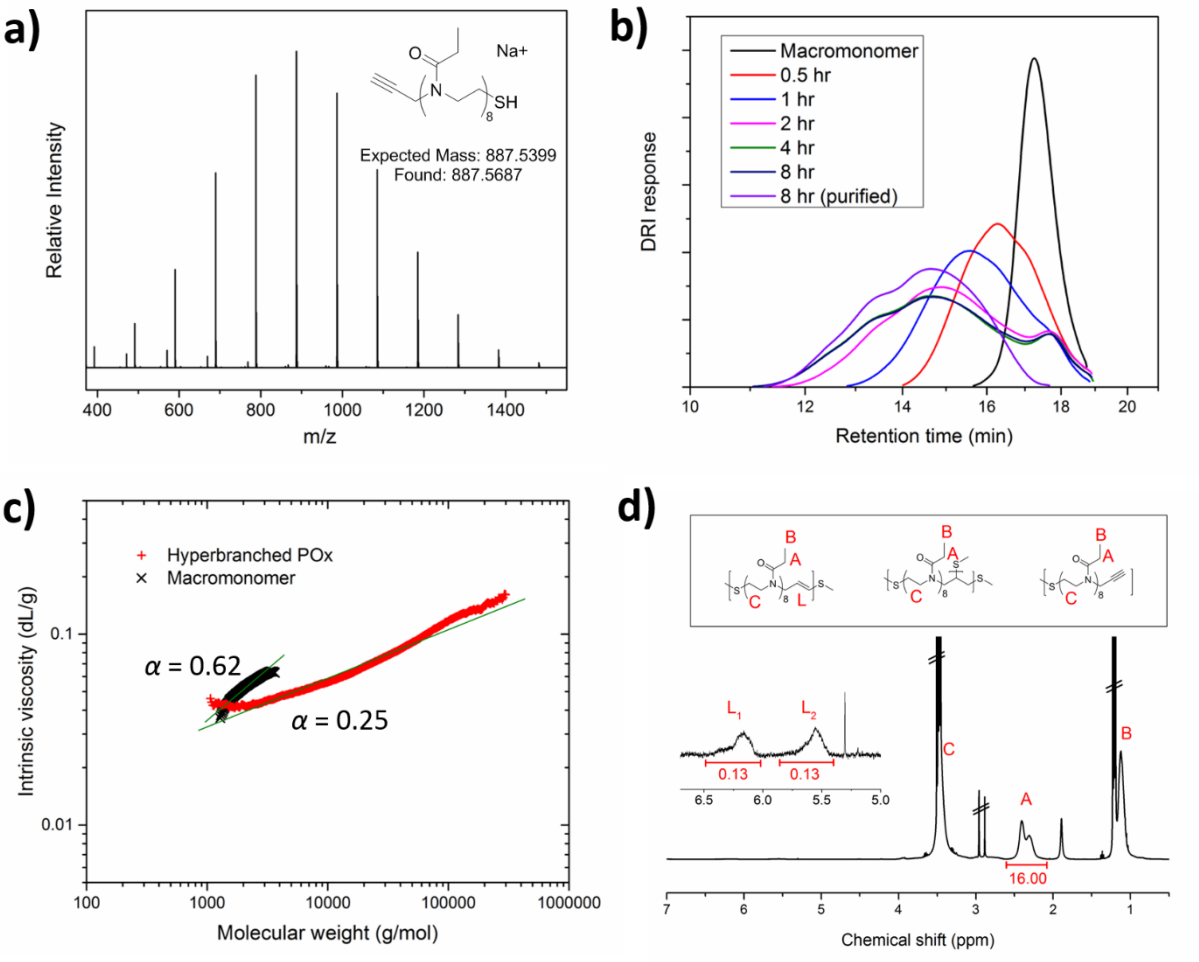

Figure 1. (a) Size-exclusion chromatograms (normalised DRI detector response vs retention time) of the photopolymerisation of PEtOx thiol-yne macromonomer following various irradiation time. (b) ESI mass spectra of telechelic PEtOx thiol-yne macromonomer. (c) Kuhn-Mark-Houwink-Sakurada (KMHS) plots of log intrinsic viscosity against log molecular weight from SEC viscosity detector in DMF eluent of PEtOx thiol-yne macromonomer and hyperbranched PEtOx. (d) ^{1}H NMR spectrum of hyperbranched PEtOx showing peak assignments, inset showing zoomed view of vinyl region.

The formation of hyperbranched PEtOx was followed *via* SEC, as shown in **Figure 1b**. Upon UV irradiation, the chromatogram peak associated with the macromonomer decreases while the DRI trace shifts to shorter retention times and thus higher molecular weights. In addition, a broadening of the chromatograms with increasing reaction time, due to the step growth nature of the thiol-yne polymerisation, was detected. Values for molecular weight and dispersity of the polymerisation kinetic study are summarised in **Table S2**. The M_n values reported correspond to SEC measurements compared to linear polymer calibration standards, which is expected to significantly underestimate the value as hyperbranched polymers have smaller hydrodynamic radii than their equivalent linear polymers. **Figure 1c** shows the Kuhn-Mark-Houwink-Sakurada plots of intrinsic viscosity against molecular weight for both the macromonomer and the final hyperbranched PEtOx after purification. The gradient of the lines, referred to as α, indicates the branched nature of the final polymer. With more branching, a polymer is typically involved in fewer chain entanglements, resulting in reduced increase of the viscosity with increasing molecular weight (for linear polymers, α value is typically 0.6 - 0.8). The α values of 0.62 for the linear macromonomer and 0.25 for the hyperbranched PEtOx illustrate the high density of branching. The degree of branching, as described by Hawker,[29] can be calculated from the integral of the linear units in the ^{1}H NMR spectra which can be identified at around 6-6.5 ppm (**Figure 1d**, **Figure S7, Table S1**).

Table 1. Copolymer compositions, molecular weights, dispersity, and hydrodynamic radius values for both linear PEtOx and hyperbranched thiol–yne polymers prepared by photopolymerisation of PEtOx thiol-yne macromonomers.

	Sample	% PEI [a]	% PEtOx [a]	$M_{n\ NMR}$ (g/mol) [a]	$M_{n\ GPC}$ (g/mol) [b]	$Đ$ [b]	$R_{h\ SLS}$ (nm) [c]	$M_{w\ SLS}$ (g/mol) [c]
	PEtOx macromonomer	0	100	800	1,200	1.19	-	-
	Hyperbranched PEtOx	0	100	17,100	14,000	1.5	3.6	20,400
HB 32%	Hyperbranched P($EI_{0.32}$-*co*-$EtOx_{0.68}$)	32	68	14,100	-	-	6.8	21,900
HB 58%	Hyperbranched P($EI_{0.58}$-*co*-$EtOx_{0.42}$)	58	42	12,500	-	-	8.1	65,300
HB 76%	Hyperbranched P($EI_{0.76}$-*co*-$EtOx_{0.24}$)	76	24	10,900	-	-	8.6	106,200
	Linear PEtOx	0	100	15,800	13,700	1.25	4.2	19,100
L 81%	Linear P($EI_{0.81}$-*co*-$EtOx_{0.19}$)	81	19	9,200	-	-	54.0	12,400

[a] Determined by ^{1}H NMR spectroscopy. [b] From DMF SEC with DRI detector and PMMA standard. [c] From SLS in water (further SLS details in Supplementary Info).

To create polymers able to interact with genetic material, cationic charges have to be introduced into the structure. In the present case, this is done using partial hydrolysis of the repeating unit of PEtOx, creating poly(ethylenimine) units along the polymer backbone. Hydrolysis of hyperbranched PEtOx was carried out in 1M aqueous solution of HCl at 120 °C. Microwave irradiation was chosen as the heating method of choice as it allows for increased pressure, thus reducing reaction times.[30] These hydrolysis conditions allow control over the rate and degree of hydrolysis. A kinetic study, in which the hydrolysis is determined from analysing the increase of the integral of the hydrolysed propionic acid small molecule over time in ^{1}H-NMR spectra, was undertaken with both hyperbranched PEtOx and linear PEtOx (**Figure S9**). Interestingly, the branched structure does not appear to affect the hydrolysis rate of the EtOx side chains (**Figure S8**). Using this method, three hyperbranched poly(ethylenimine-*co*-oxazoline) copolymers were produced. The final composition of the three hyperbranched copolymers was calculated from the integrals of CH_2 groups from the polyethylenimine backbone and the CH_2 groups from the polyoxazoline backbone, between 2.5 ppm and 3.5 ppm (**Figure 2b**).

Copolymers were analysed by SEC (**Table 1**). Resulting chromatograms show a monomodal size distribution for all polymers (**Figure S10**) with varying values for M_n. SEC characterisation of highly charged polymers is often complicated by non-size exclusion interferences, such as intramolecular electrostatic interactions, column adsorption, or ion exchange effects, which are known to cause increased retention times and poor chromatographic peak shape, resulting in large errors in molecular weight estimation.[31-33] Therefore, static light scattering was employed to further investigate the molecular weight of the synthesized poly(ethylenimine-*co*-oxazoline) copolymers, as well as poly(2-ethyl-2-oxazoline) precursor materials (**Figures S11-S16**). SLS is generally a good complementary method of molecular weight determination for hyperbranched polymers as it does not rely on calibration. However, the molecular weights obtained from SLS measurement show an unexpected increase with increasing degree of hydrolysis. This can be attributed to the presence of a combination of closely-spaced protonated amines and a hydrophobic backbone, which can lead to solution polyelectrolyte states that shift between aggregated and free forms.[34] Hydrodynamic radii obtained for SLS agreed with what would be expected for hyperbranched polymers. The hyperbranched PEtOx was found to have a hydrodynamic radius of 3.6 nm, which increased to 6.8, 8.1, and 8.6 nm with increasing degrees of hydrolysis. The increase can be attributed to swelling of poly(ethylenimine-*co*-oxazoline) in water with increasing charge content. For comparison, a linear polymer control of equivalent molecular weight was synthesised by CROP of EtOx ($M_{n,SEC}$ 14,000 g/mol, $Đ$ 1.25). The linear control was hydrolysed using the previously described methodology to yield poly(ethylenimine-*co*-oxazoline) with a degree of hydrolysis similar to that of the hyperbranched copolymer with the highest PEI content.

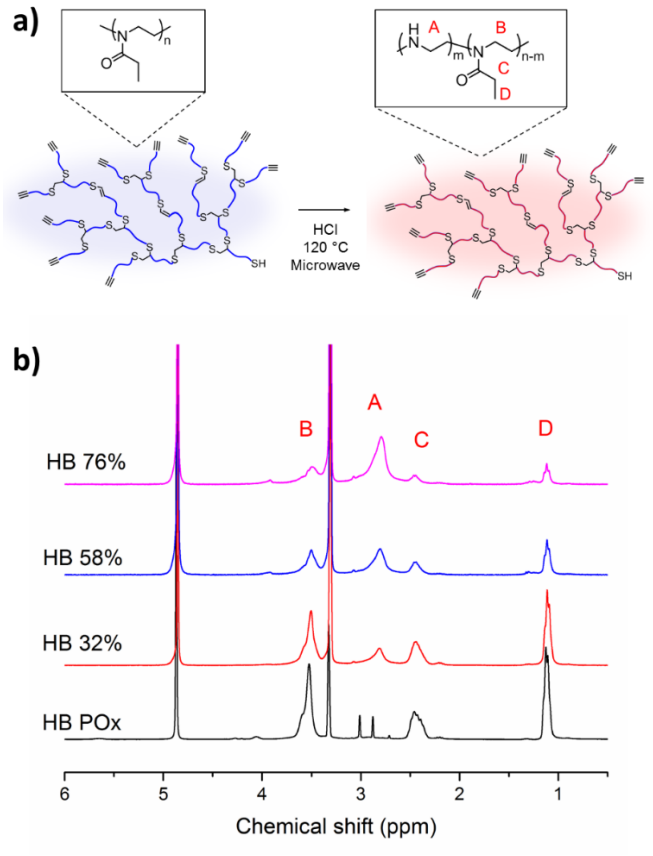

Figure 2. a) Schematic representation of the acid-catalysed hydrolysis of hyperbranched poly(2-ethyl-2-oxazoline) polymer into hyperbranched poly(ethylenimine-co-oxazoline) copolymers; **b)** ^{1}H NMR spectra of final hyperbranched poly(ethylenimine-co-oxazoline) copolymers, showing peaks used for calculation of the composition.

Effect of type of amine and branching on polymer buffering capacity

Successful gene expression in target cells requires escape of polyplexes from the endosomal/lysosomal pathway after cell internalisation.[35] For PEI polyplexes, this is assumed to occur *via* the 'proton sponge' effect, although this still receives considerable debate.[36-38] In brief, the abundance of amines groups in PEI results in a high buffering capacity of the polymers, which is thought to cause an increase in lysosomal pH as protons are pumped into the lysosome from the cytosol. A combination of PEI swelling due to electrostatic repulsion of protonated amine groups, and osmotic pressure change in the vesicles is expected to cause interruption and rupture of the lysosomal membrane, releasing the polyplex into the cytosol. In the present study, for the first time hyperbranched PEI structures containing only secondary amines are used, allowing observation of the influence of architecture on the performance of the polymers isolated from the nature of the amines. To evaluate the buffering effect of hyperbranched poly(ethylenimine-*co*-oxazoline) and compare it to that of PEI, pH titrations were carried out by addition of NaOH solution into solutions of the acidified polymers (**Figure 3**). The titration of bPEI shows a very broad change in pH transition (between 0.2 - 1 mmol/dm^3 of NaOH added), which is expected from a polymer containing amine groups with the three different pK_a values. In contrast, ethylenimine oxazoline copolymers showed a sharper titration curve, with a pH transition occurring between 0.3 – 0.5 mmol/dm^3 of NaOH added, which can be attributed to the presence of secondary amine groups only. Most importantly, the negligible difference between the titration curves of linear and hyperbranched PEI structures shows that, indeed the polymer architecture has only a low influence on the overall pK_a values,which makes the presented polymers an ideal platform to study the impact of polymer architecture on transfection. These results support our hypothesis that hyperbranched poly(ethylenimine-*co*-oxazoline) could be an interesting candidate for non-viral gene delivery applications as it shows characteristics of linear PEI but with an globular hyperbranched polymer architecture.

Polymer-pDNA complexation and resulting particle morphology

The ability of hyperbranched and linear poly(ethylenimine-*co*-oxazoline) to bind GFP plasmid DNA was first assessed using agaraose gel electrophoresis. Polymers were complexed with pDNA at varying N/P ratios (ratio of positively charged nitrogen groups on polymer to negatively charged phosphate groups on DNA). Images of the resulting agarose gels are shown in **Figure 4a**. As expected, hyperbranched poly(ethylenimine-*co*-oxazoline) with a degree of hydrolysis of 32% shows moderate ability to bind nucleic acids, with free pDNA still detectable at N/P ratio as high as 20. With a degree of hydrolysis of 58%, the polymer is able to fully complex

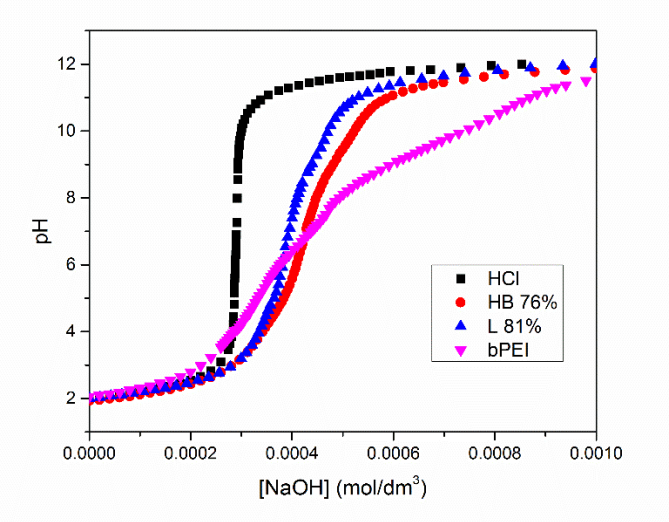

Figure 3. pH titration experiments for hyperbranched poly(ethylenimine-co-oxazoline) copolymer (76% hydrolysed), linear equivalent (81% hydrolysed) as well as commercial branched PEI. A control of NaOH titration into HCl acid is shown for reference.

pDNA at an N/P ratio of 10 to 20. Hyperbranched poly(ethylenimine-*co*-oxazoline) with a degree of hydrolysis of 76%, its linear equivalent, and the commercial bPEI all show formation of polyplexes and full binding of free pDNA at an N/P ratio of 5 to 10.

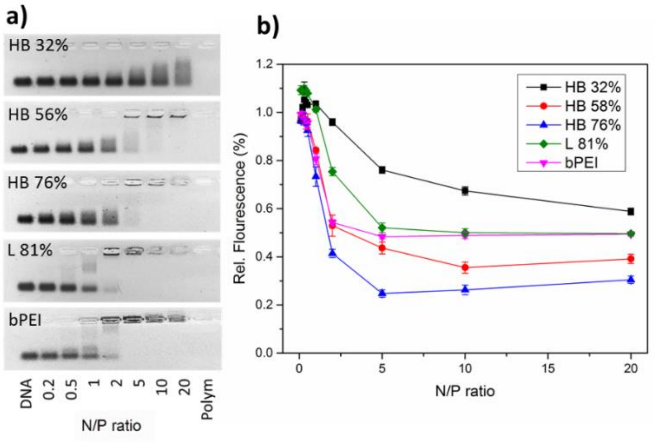

Figure 4. a) Polyplex formation with pDNA, as characterised by agarose gel electrophoresis using the various PEI polymers; **b)** Ethidium bromide displacement assay, as a complimentary technique to characterise polymer ability to complex pDNA.

A complimentary method to characterise DNA/RNA binding relies on competitive displacement of ethidium bromide, bound to DNA, by cationic polymers. A reduced fluorescence is observed when ethidium bromide is excluded from binding sites located in the groove of the oligonucleotides, due to addition of polymer.[39] The results, shown in **Figure 4B**, show a decrease in fluorescence intensity with increasing N/P ratio, typical of polyplex formation. A number of trends can be observed in this data: (i) For hyperbranched poly(ethylenimine-*co*-oxazoline), pDNA binding ability increases with increasing amine content from 32% to 58% and to 76%, which is in agreement with the results of the gel electrophoresis, (ii) linear poly(ethylenimine-*co*-oxazoline) binds to pDNA less strongly than the equivalent hyperbranched polymer, (iii) hyperbranched poly(ethylenimine-*co*-oxazoline) 76% binds more strongly than bPEI.

In addition, the presence of a plateau of residual fluorescence indicates the presence of remaining intercalated ethidium bromide which cannot be displaced. This is especially apparent in the case of hyperbranched p($EI_{0.32}$-*co*-$EtOx_{0.68}$), linear p($EI_{0.81}$-*co*-$EtOx_{0.19}$), and commercial bPEI. This phenomenon is due to the polymers forming complexes in which fewer amines are available to interact with pDNA, and displace ethidium bromide. In the case of the linear polymer, its extended conformation is expected to result in looser and larger complexes. In the case of bPEI, the presence of tertiary amines which are not protonated at pH ~7, is expected to weaken the complexation of pDNA. This result highlights the importance of precise understanding polymer and pDNA interactions, and prompt a more thorough characterisation of the polyplex formed.

Table 2. Size and surface charge (zetapotential) of polyplexes formed with pDNA at both N/P = 20 and N/P = 40, as determined by dynamic light scattering and electrophoretic light scattering.

	N/P ratio	Z-average size (d.nm)	PDI	Zetapotential (mV)
HB 32%	20	499.6	0.18	5.4 ±0.421
	40	419.7	0.14	7.3 ±0.572
HB 58%	20	64.6	0.27	22.3 ±1.75
	40	72.3	0.36	24.3 ±1.91
HB 76%	20	53.6	0.36	24.4 ±1.91
	40	71.9	0.41	25.5 ±2.00
bPEI	20	82.3	0.51	39.7 ±3.11
	40	85.6	0.54	39.4 ±3.09
L 81%	20	246.7	0.36	45.9 ±3.60
	40	514.3	0.51	45.6 ±3.78

To further investigate the influence of polymer architecture on pDNA binding, polyplex physical characteristics were determined using dynamic light scattering and zetapotential measurements, to elucidate size and surface charge properties. Previous studies indicate that efficient cellular uptake occurs for particles typically between 50 to 200 nm in size. Excess positive charge was also demonstrated to enhance cellular uptake.[40] Table 2 shows the size and surface charge of the various polyplexes formed. For hyperbranched poly(ethylenimine-*co*-oxazoline), diameters follow a trend similar to the ethidium bromide assay, with size of the particles decreasing as the amine content increases from 32% to 58% and to 76%. Linear poly(ethylenimine-*co*-oxazoline) polyplexes appear to form slightly larger particles, which can be attributed to the weaker DNA binding strength of the polymer when compared to the hyperbranched equivalent, as well as potential intermolecular crosslinking of DNA molecules with the extended linear polymer.

AFM imaging of polymer pDNA complexes was carried out to complement the size measurements obtained using DLS (**Figure 5 and S17-S20**). Uncomplexed plasmid DNA deposited on a mica surface is distributed in a network type of structure. This is consistent with previous reports of uncondensed DNA morphologies in the literature.[41,42] In samples where the pDNA was previously mixed with hyperbranched p($EI_{0.76}$-*co*-$EtOx_{0.24}$), polyplexes with a size of approximately 100 nm were observed. A similar structure was obtained using the commercial branched PEI. Similarly to DLS data, polyplexes formed with

linear p($EI_{0.81}$-*co*-$EtOx_{0.19}$) showed a size of approximately 200 nm instead. Furthermore, branched PEI and small cyclic polycations have previously been reported to more effectively condense DNA.[19,43] For example, Li *et al.* found that linear polycations/DNA complexes form larger aggregates than the cyclic polymer equivalent, which was attributed to the stretched conformation being able to intermolecularly crosslink DNA molecules.[44] Taken together, these data demonstrate the fundamental influence of polymer architecture on DNA complexation and polyplex formation.

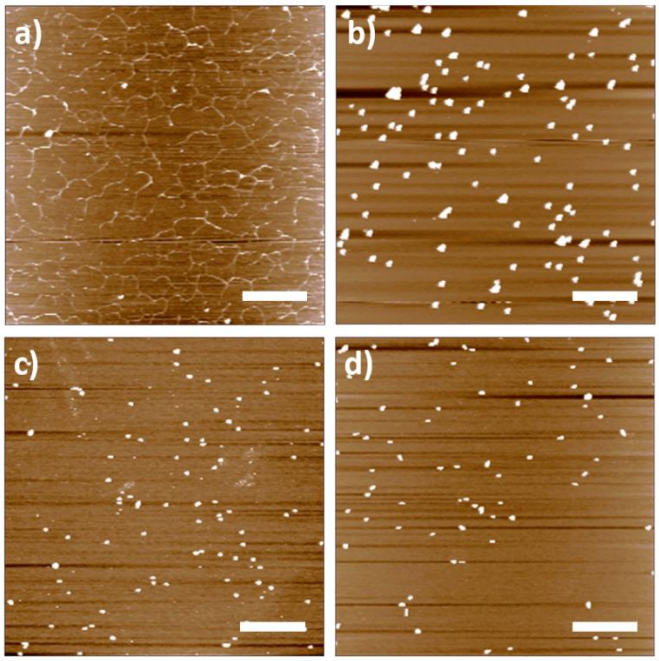

Figure 5. AFM images of polyplex morphology at N/P = 20, **a)** pDNA only, **b)** L 81% polyplex, **c)** HB 76% polyplex, **d)** bPEI polyplex. Each scan represents an area of 10 µm by 10 µm. Scale bars all 2 µm.

Effect of polymer architecture on toxicity and pDNA transfection *in-vitro*

A common limitation of cationic polymers is their ability to permeabilise cellular membranes.[45,46] Here, toxicity of the polymers was assessed using the XTT assay on human embryo kidney cells HEK293T as model (**Figure 6a**). Polymer toxicity studies confirmed that commercial bPEI is toxic at concentrations as low as 0.2 mg/mL. In contrast, cells treated with poly(ethylenimine-*co*-oxazoline) polymers were found to have viability of over 80 % at concentration up to 0.8 mg/mL, which is far above the relevant concentrations used both *in vitro* and *in vivo*.[47] At higher polymer concentrations (>2 mg/mL), hyperbranched p($EI_{0.76}$-*co*-$EtOx_{0.24}$) becomes slightly toxic, whereas the linear equivalent polymer causes complete cell death at the same concentration. The reduced toxicity of the hyperbranched architecture compared to the linear architecture follows similar observations made for branched/linear polymers of alternative monomers.[48,49] We attribute this to differences in the 3D structure and flexibility of the polymers, resulting in different interaction of the polymers with the cell surface. It was previously shown that rigid polymers interact with lipid membranes with more difficulty than flexible equivalents.[50] Thus, it appears reasonable that the less flexible hyperbranched poly(ethylenimine-*co*-oxazoline) show decreased toxicity as compared to its flexible linear equivalent.

Transfection of plasmid DNA containing GFP reporter gene using the polymers prepared in this study was evaluated on transfectable derivative of human embryonic kidney (HEK293T) cell line as model (**Figure 6b**) and reported relative to commercial bPEI. Cellular fluorescence histograms, obtained by flow cytometry following 5 hours of cell incubation with the polyplexes followed by 24 hours of subsequent growth, were used to determine transfection efficiencies (**Figure S21**). An N/P ratio of 20 was chosen for the transfection studies in order to have sufficient polymer to bind the plasmid even for copolymer samples with lower percentages of PEI. In the case of hyperbranched p($EI_{0.32}$-*co*-$EtOx_{0.68}$), transfection efficiencies only 2.5 fold better than naked pDNA were obtained, which can be attributed to incomplete complexation of the pDNA at this N/P ratio. Hyperbranched p($EI_{0.58}$-*co*-$EtOx_{0.42}$) showed a relatively similar transfection efficiency (around 6 fold better than naked pDNA). Accordingly, in the case of hyperbranched p($EI_{0.76}$-*co*-$EtOx_{0.24}$) and linear p($EI_{0.81}$-*co*-$EtOx_{0.19}$) copolymers where the degree of oxazoline hydrolysis is higher, transfection efficiencies reach values of 75% that of bPEI. The observed difference in transfection between the hyperbranched p($EI_{0.76}$-*co*-$EtOx_{0.24}$) and linear p($EI_{0.81}$-*co*-$EtOx_{0.19}$) copolymers is minimal, however further work will focus on variation of molecular weight, and higher percentages of ethylenimine, to further uncover any architectural differences of these copolymers as non-viral vectors. The polymers reaching similar transfections as commercial bPEI is a noteworthy result when also taking into account the much reduced toxicity of the thiol-yne hyperbranched polymer, and suggests these materials are ideal candidates as lower toxicity alternatives to PEI.

When considering transfection mechanisms in relation to the synthesised polymers, the degree of impact of the polymer buffering capacity on endosomal escape and transfection is unclear. It has more recently be shown that free polymer chains can have an impact gene transfection.[51-53] Whereby the mechanism of cationic polymer mediated plasmid transfection, could be explained by free polymer interaction with the interior endosomal membrane and creation of pores, allowing an amount of polyplex into the cytoplasm. Any small change in the transfection process could have disproportionate effect on observed expression due to endosome escape being very inefficient.[54] To our knowledge there has been no published research on the impact of the free polymer chain architecture on possible endosome escape, which highlights the benefit of having controlled polymer architectures. The degree of substitution of the amines could also play a role; only a handful of studies have investigated this.[55-57] Having comparable

branched and linear PEI systems with the same amine substitution patterns is important.

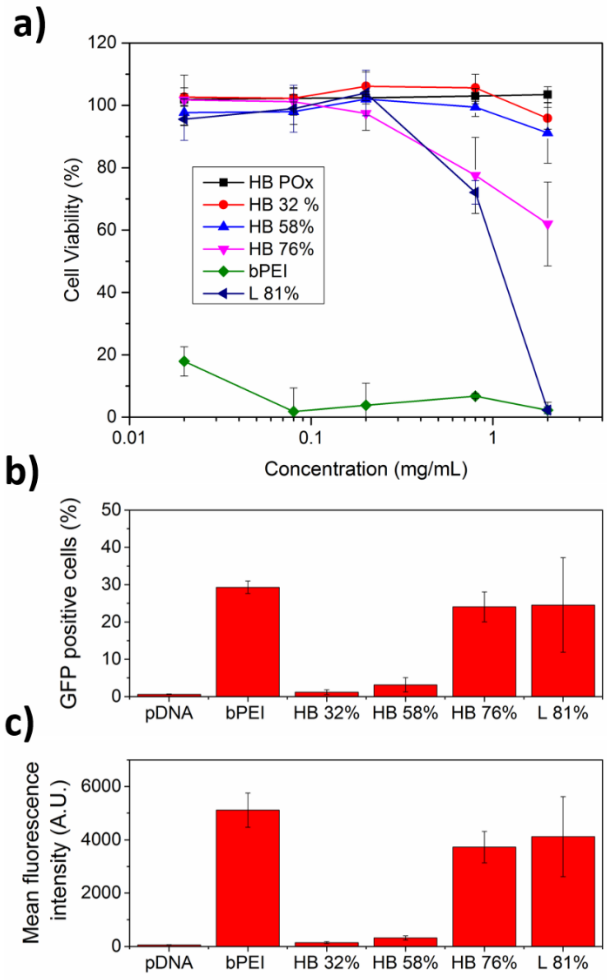

Figure 6. a) Cell viability as determined using XTT assay on human embryo kidney cells HEK293T treated with hyberbranched poly(ethyleneimine-co-oxazoline) copolymers, linear poly(ethyleneimine-co-oxazoline) copolymer, and bPEI for 24 hours at 37 °C; **b)** and **c)** GFP plasmid DNA transfection in HEK293T cell-line following 5 hours polyplex incubation (N/P 20, 10 μg/mL DNA concentration in well) and 24 hours subsequent growth. Intracellular fluorescence was determined by flow cytometry.

Conclusions

Synthesis of hyperbranched poly(ethylenimine-*co*-oxazoline) by AB_2 thiol-yne photo-addition chemistry is reported for the first time. This synthetic route allows for the preparation of hyperbranched polymers from macromolecular monomer units, with degrees of branching in the region of dendrimers. In contrast with the mixture of amines and uncontrolled patterns typically obtained by the synthesis of branched PEI *via* the ring opening polymerisation of aziridine, the method presented here results in hyperbranched PEI structures containing only secondary amines and well defined branching patterns. Hyperbranched poly(ethylenimine-*co*-oxazoline) and bPEI were found to complex GFP plasmid DNA to form positively charged particles. In comparison, linear forms were found to form larger aggregates. Differences were also found in polymer *in vitro* cytotoxicity, with poly(ethylenimine-*co*-oxazoline)s having reduced toxicity compared to bPEI, and the hyperbranched poly(ethylenimine-*co*-oxazoline) having reduced toxicity compared to the linear equivalent. Delivery of pDNA encoding for GFP showed that poly(ethylenimine-*co*-oxazoline) copolymers with high percentages of ethylenimine units were have transfection efficiencies slightly lower than the commercial standard 25K branched PEI. When considering this in conjunction with the lower toxicities, the hyperbranched poly(ethylenimine-*co*-oxazoline) represents an promising candidate for further non-viral gene delivery studies. In agreement with the literature, it is believed that the compact hyperbranched polymer conformation contributes, in some extent, to the improved toxicity. The synthesised hyperbranched PEI copolymers highlight the importance of understanding polymer architecture when developing gene delivery systems.

Associated content

Further experimental section details of light scattering measurements, zetapotential measurements, and AFM imaging; ^{1}H NMR spectroscopy spectra, size exclusion chromatograms, representative degree of branching calculations, hydrolysis kinetic data, light scattering characterisation data, further AFM images, and flow cytometry data.

Acknowledgments

The Royal Society Wolfson Merit Award (WM130055; S.P.), Monash-Warwick Alliance (S.P., J.Z.), and Syngenta (A.C.) are acknowledged for financial support. The European Research Council (TUSUPO 647106; S.P., R.P.), the German Research Foundation (DFG, GZ: HA 7725/1-1; M.H.), and the Engineering and Physical Sciences Research Council (EP/F500378/1; J.T.) are gratefully acknowledged for funding. The authors would like to thank Dr Daniel Lester and the University of Warwick Polymer Characterisation Research Technology Platform (RTP) for GPC facilities.

References

(1) Somia, N.; Verma, I. M., Gene therapy: Trials and tribulations, *Nature Reviews Genetics* **2000**, *1*, 91.
(2) Putnam, D., Polymers for gene delivery across length scales, *Nat. Mater.* **2006**, *5*, 439.
(3) Griesenbach, U.; Alton, E., Gene transfer to the lung: Lessons learned from more than 2 decades of CF gene therapy, *Adv. Drug Del. Rev.* **2009**, *61*, 128.

(4) Johnson, L. A.; Morgan, R. A.; Dudley, M. E.; Cassard, L.; Yang, J. C.; Hughes, M. S.; Kammula, U. S.; Royal, R. E.; Sherry, R. M.; Wunderlich, J. R.; Lee, C. C. R.; Restifo, N. P.; Schwarz, S. L.; Cogdill, A. P.; Bishop, R. J.; Kim, H.; Brewer, C. C.; Rudy, S. F.; VanWaes, C.; Davis, J. L.; Mathur, A.; Ripley, R. T.; Nathan, D. A.; Laurencot, C. M.; Rosenberg, S. A., Gene therapy with human and mouse T-cell receptors mediates cancer regression and targets normal tissues expressing cognate antigen, *Blood* **2009**, *114*, 535.

(5) Maguire, A. M.; High, K. A.; Auricchio, A.; Wright, J. F.; Pierce, E. A.; Testa, F.; Mingozzi, F.; Bennicelli, J. L.; Ying, G. S.; Rossi, S.; Fulton, A.; Marshall, K. A.; Banfi, S.; Chung, D. C.; Morgan, J. I. W.; Hauck, B.; Zelenaia, O.; Zhu, X. S.; Raffini, L.; Coppieters, F.; De Baere, E.; Shindler, K. S.; Volpe, N. J.; Surace, E. M.; Acerra, C.; Lyubarsky, A.; Redmond, T. M.; Stone, E.; Sun, J. W.; McDonnell, J. W.; Leroy, B. P.; Simonelli, F.; Bennett, J., Age-dependent effects of RPE65 gene therapy for Leber's congenital amaurosis: a phase 1 dose-escalation trial, *Lancet* **2009**, *374*, 1597.

(6) Kaplitt, M. G.; Feigin, A.; Tang, C.; Fitzsimons, H. L.; Mattis, P.; Lawlor, P. A.; Bland, R. J.; Young, D.; Strybing, K.; Eidelberg, D.; During, M. J., Safety and tolerability of gene therapy with an adeno-associated virus (AAV) borne GAD gene for Parkinson's disease: an open label, phase I trial, *Lancet* **2007**, *369*, 2097.

(7) Bowles, D. E.; McPhee, S. W. J.; Li, C. W.; Gray, S. J.; Samulski, J. J.; Camp, A. S.; Li, J.; Wang, B.; Monahan, P. E.; Rabinowitz, J. E.; Grieger, J. C.; Govindasamy, L.; Agbandje-McKenna, M.; Xiao, X.; Samulski, R. J., Phase 1 Gene Therapy for Duchenne Muscular Dystrophy Using a Translational Optimized AAV Vector, *Mol. Ther.* **2012**, *20*, 443.

(8) Jinek, M.; Chylinski, K.; Fonfara, I.; Hauer, M.; Doudna, J. A.; Charpentier, E., A Programmable Dual-RNA-Guided DNA Endonuclease in Adaptive Bacterial Immunity, *Science* **2012**, *337*, 816.

(9) Cong, L.; Ran, F. A.; Cox, D.; Lin, S. L.; Barretto, R.; Habib, N.; Hsu, P. D.; Wu, X. B.; Jiang, W. Y.; Marraffini, L. A.; Zhang, F., Multiplex Genome Engineering Using CRISPR/Cas Systems, *Science* **2013**, *339*, 819.

(10) Yin, H.; Kanasty, R. L.; Eltoukhy, A. A.; Vegas, A. J.; Dorkin, J. R.; Anderson, D. G., Non-viral vectors for gene-based therapy, *Nature Reviews Genetics* **2014**, *15*, 541.

(11) Cook, A. B.; Peltier, R.; Hartlieb, M.; Whitfield, R.; Moriceau, G.; Burns, J. A.; Haddleton, D. M.; Perrier, S., Cationic and hydrolysable branched polymers by RAFT for complexation and controlled release of dsRNA, *Polymer Chemistry* **2018**, *9*, 4025.

(12) Cook, A. B.; Peltier, R.; Barlow, T. R.; Tanaka, J.; Burns, J. A.; Perrier, S., Branched poly(trimethylphosphonium ethylacrylate-co-PEGA) by RAFT: alternative to cationic polyammoniums for nucleic acid complexation, *Journal of Interdisciplinary Nanomedicine* **2018**, *In Press*, doi:10.1002/jin2.50

(13) Fischer, D.; Bieber, T.; Li, Y. X.; Elsasser, H. P.; Kissel, T., A novel non-viral vector for DNA delivery based on low molecular weight, branched polyethylenimine: Effect of molecular weight on transfection efficiency and cytotoxicity, *Pharm. Res.* **1999**, *16*, 1273.

(14) Anderson, D. G.; Akinc, A.; Hossain, N.; Langer, R., Structure/property studies of polymeric gene delivery using a library of poly(beta-amino esters), *Mol. Ther.* **2005**, *11*, 426.

(15) Intra, J.; Salem, A. K., Characterization of the transgene expression generated by branched and linear polyethylenimine-plasmid DNA nanoparticles in vitro and after intraperitoneal injection in vivo, *J. Control. Release* **2008**, *130*, 129.

(16) Goula, D.; Remy, J. S.; Erbacher, P.; Wasowicz, M.; Levi, G.; Abdallah, B.; Demeneix, B. A., Size, diffusibility and transfection performance of linear PEI/DNA complexes in the mouse central nervous system, *Gene Ther.* **1998**, *5*, 712.

(17) Wightman, L.; Kircheis, R.; Rossler, V.; Carotta, S.; Ruzicka, R.; Kursa, M.; Wagner, E., Different behavior of branched and linear polyethylenimine for gene delivery in vitro and in vivo, *J. Gene Med.* **2001**, *3*, 362.

(18) Tang, M. X.; Redemann, C. T.; Szoka, F. C., In vitro gene delivery by degraded polyamidoamine dendrimers, *Bioconjugate Chem.* **1996**, *7*, 703.

(19) Godbey, W. T.; Wu, K. K.; Mikos, A. G., Poly(ethylenimine) and its role in gene delivery, *J. Control. Release* **1999**, *60*, 149.

(20) Cortez, M. A.; Godbey, W. T.; Fang, Y. L.; Payne, M. E.; Cafferty, B. J.; Kosakowska, K. A.; Grayson, S. M., The Synthesis of Cyclic Poly(ethylene imine) and Exact Linear Analogues: An Evaluation of Gene Delivery Comparing Polymer Architectures, *J. Am. Chem. Soc.* **2015**, *137*, 6541.

(21) Konkolewicz, D.; Gray-Weale, A.; Perrier, S., Hyperbranched Polymers by Thiol-Yne Chemistry: From Small Molecules to Functional Polymers, *J. Am. Chem. Soc.* **2009**, *131*, 18075.

(22) Cook, A. B.; Barbey, R.; Burns, J. A.; Perrier, S., Hyperbranched Polymers with High Degrees of Branching and Low Dispersity Values: Pushing the Limits of Thiol–Yne Chemistry, *Macromolecules* **2016**, *49*, 1296.

(23) Hartlieb, M.; Floyd, T.; Cook, A. B.; Sanchez-Cano, C.; Catrouillet, S.; Burns, J. A.; Perrier, S., Well-defined hyperstar copolymers based on a thiol-yne hyperbranched core and a poly(2-oxazoline) shell for biomedical applications, *Polymer Chemistry* **2017**, *8*, 2041.

(24) Barbey, R.; Perrier, S., Synthesis of Polystyrene-Based Hyperbranched Polymers by Thiol-Yne Chemistry: A Detailed Investigation, *Macromolecules* **2014**, *47*, 6697.

(25) Bus, T.; Englert, C.; Reifarth, M.; Borchers, P.; Hartlieb, M.; Vollrath, A.; Hoeppener, S.; Traeger, A.; Schubert, U. S., 3rd generation poly(ethylene imine)s for gene delivery, *J. Mater. Chem. B* **2017**, *5*, 1258.

(26) Rinkenauer, A. C.; Tauhardt, L.; Wendler, F.; Kempe, K.; Gottschaldt, M.; Traeger, A.; Schubert, U. S., A Cationic Poly(2-oxazoline) with High In Vitro Transfection Efficiency Identified by a Library Approach, *Macromol. Biosci.* **2015**, *15*, 414.

(27) Hartlieb, M.; Kempe, K.; Schubert, U. S., Covalently cross-linked poly(2-oxazoline) materials for biomedical applications - from hydrogels to self-assembled and templated structures, *J. Mater. Chem. B* **2015**, *3*, 526.

(28) Fairbanks, B. D.; Scott, T. F.; Kloxin, C. J.; Anseth, K. S.; Bowman, C. N., Thiol-Yne Photopolymerizations: Novel Mechanism, Kinetics, and Step-Growth Formation of Highly Cross-Linked Networks, *Macromolecules* **2009**, *42*, 211.

(29) Hawker, C. J.; Lee, R.; Frechet, J. M. J., One-step synthesis of hyperbranched dendritic polyesters, *J. Am. Chem. Soc.* **1991**, *113*, 4583.
(30) de la Rosa, V. R.; Bauwens, E.; Monnery, B. D.; De Geest, B. G.; Hoogenboom, R., Fast and accurate partial hydrolysis of poly(2-ethyl-2-oxazoline) into tailored linear polyethylenimine copolymers, *Polymer Chemistry* **2014**, *5*, 4957.
(31) Dubin, P. In *Journal of Chromatography Library*; Dubin, P. L., Ed.; Elsevier: 1988; Vol. Volume 40, p xiii.
(32) Perevyazko, I.; Gubarev, A. S.; Tauhardt, L.; Dobrodumov, A.; Pavlov, G. M.; Schubert, U. S., Linear poly(ethylene imine)s: true molar masses, solution properties and conformation, *Polymer Chemistry* **2017**, *8*, 7169.
(33) Striegel, A. M.; Yau, W. W.; Kirkland, J. J.; Bly, D. D. In *Modern Size-Exclusion Liquid Chromatography*; John Wiley & Sons, Inc.: 2009, p i.
(34) Curtis, K. A.; Miller, D.; Millard, P.; Basu, S.; Horkay, F.; Chandran, P. L., Unusual Salt and pH Induced Changes in Polyethylenimine Solutions, *PLoS One* **2016**, *11*.
(35) Niidome, T.; Huang, L., Gene therapy progress and prospects: Nonviral vectors, *Gene Ther.* **2002**, *9*, 1647.
(36) Benjaminsen, R. V.; Mattebjerg, M. A.; Henriksen, J. R.; Moghimi, S. M.; Andresen, T. L., The Possible "Proton Sponge" Effect of Polyethylenimine (PEI) Does Not Include Change in Lysosomal pH, *Mol. Ther.* **2013**, *21*, 149.
(37) Akinc, A.; Thomas, M.; Klibanov, A. M.; Langer, R., Exploring polyethylenimine-mediated DNA transfection and the proton sponge hypothesis, *J. Gene Med.* **2005**, *7*, 657.
(38) Behr, J. P., The proton sponge: A trick to enter cells the viruses did not exploit, *Chimia* **1997**, *51*, 34.
(39) Tse, W. C.; Boger, D. L., A fluorescent intercalator displacement assay for establishing DNA binding selectivity and affinity, *Acc. Chem. Res.* **2004**, *37*, 61.
(40) Frohlich, E., The role of surface charge in cellular uptake and cytotoxicity of medical nanoparticles, *International Journal of Nanomedicine* **2012**, *7*, 5577.
(41) Zhao, X.; Cui, H. X.; Chen, W. J.; Wang, Y.; Cui, B.; Sun, C. J.; Meng, Z. G.; Liu, G. Q., Morphology, Structure and Function Characterization of PEI Modified Magnetic Nanoparticles Gene Delivery System, *PLoS One* **2014**, *9*.
(42) Rackstraw, B. J.; Martin, A. L.; Stolnik, S.; Roberts, C. J.; Garnett, M. C.; Davies, M. C.; Tendler, S. J. B., Microscopic investigations into PEG-cationic polymer-induced DNA condensation, *Langmuir* **2001**, *17*, 3185.
(43) Dunlap, D. D.; Maggi, A.; Soria, M. R.; Monaco, L., Nanoscopic structure of DNA condensed for gene delivery, *Nucleic Acids Res.* **1997**, *25*, 3095.
(44) Li, C.; Ma, C. Y.; Xu, P. X.; Gao, Y. X.; Zhang, J.; Qiao, R. Z.; Zhao, Y. F., Effective and Reversible DNA Condensation Induced by a Simple Cyclic/Rigid Polyamine Containing Carbonyl Moiety, *J. Phys. Chem. B* **2013**, *117*, 7857.
(45) Klemm, A. R.; Young, D.; Lloyd, J. B., Effects of polyethyleneimine on endocytosis and lysosome stability, *Biochem. Pharmacol.* **1998**, *56*, 41.
(46) Kafil, V.; Omidi, Y., Cytotoxic Impacts of Linear and Branched Polyethylenimine Nanostructures in A431 Cells, *Bioimpacts* **2011**, *1*, 23.
(47) Nomoto, T.; Fukushima, S.; Kumagai, M.; Machitani, K.; Arnida; Matsumoto, Y.; Oba, M.; Miyata, K.; Osada, K.; Nishiyama, N.; Kataoka, K., Three-layered polyplex micelle as a multifunctional nanocarrier platform for light-induced systemic gene transfer, *Nature Communications* **2014**, *5*.
(48) Synatschke, C. V.; Schallon, A.; Jerome, V.; Freitag, R.; Muller, A. H. E., Influence of Polymer Architecture and Molecular Weight of Poly(2-(dimethylamino)ethyl methacrylate) Polycations on Transfection Efficiency and Cell Viability in Gene Delivery, *Biomacromolecules* **2011**, *12*, 4247.
(49) Fischer, D.; Li, Y. X.; Ahlemeyer, B.; Krieglstein, J.; Kissel, T., In vitro cytotoxicity testing of polycations: influence of polymer structure on cell viability and hemolysis, *Biomaterials* **2003**, *24*, 1121.
(50) Singh, A. K.; Kasinath, B. S.; Lewis, E. J., Interaction of polycations with cell-surface negative charges of epithelial cells, *Biochim. Biophys. Acta* **1992**, *1120*, 337.
(51) Cai, J.; Yue, Y.; Wang, Y.; Jin, Z.; Jin, F.; Wu, C., Quantitative study of effects of free cationic chains on gene transfection in different intracellular stages, *J. Control. Release* **2016**, *238*, 71.
(52) Albuquerque, L. J. C.; de Castro, C. E.; Riske, K. A.; da Silva, M. C. C.; Muraro, P. I. R.; Schmidt, V.; Giacomelli, C.; Giacomelli, F. C., Gene Transfection Mediated by Catiomers Requires Free Highly Charged Polymer Chains To Overcome Intracellular Barriers, *Biomacromolecules* **2017**, *18*, 1918.
(53) Vaidyanathan, S.; Orr, B. G.; Banaszak Holl, M. M., Role of Cell Membrane–Vector Interactions in Successful Gene Delivery, *Acc. Chem. Res.* **2016**, *49*, 1486.
(54) Jones, C. H.; Chen, C.-K.; Ravikrishnan, A.; Rane, S.; Pfeifer, B. A., Overcoming Nonviral Gene Delivery Barriers: Perspective and Future, *Mol. Pharm.* **2013**, *10*, 4082.
(55) Zhu, C.; Jung, S.; Si, G.; Cheng, R.; Meng, F.; Zhu, X.; Park, T. G.; Zhong, Z., Cationic methacrylate copolymers containing primary and tertiary amino side groups: Controlled synthesis via RAFT polymerization, DNA condensation, and in vitro gene transfection, *J. Polym. Sci., Part A: Polym. Chem.* **2010**, *48*, 2869.
(56) Sprouse, D.; Reineke, T. M., Investigating the Effects of Block versus Statistical Glycopolycations Containing Primary and Tertiary Amines for Plasmid DNA Delivery, *Biomacromolecules* **2014**, *15*, 2616.
(57) Trützschler, A.-K.; Bus, T.; Reifarth, M.; Brendel, J. C.; Hoeppener, S.; Traeger, A.; Schubert, U. S., Beyond Gene Transfection with Methacrylate-Based Polyplexes—The Influence of the Amino Substitution Pattern, *Bioconjugate Chem.* **2018**, *29*, 2181.

TOC